Theor. Appl. Climatol. 78, 157–175 (2004)
DOI 10.1007/s00704-004-0050-y

Theoretical and Applied Climatology
Printed in Austria

[1] Hadley Centre for Climate Prediction & Research, Met Office, Exeter, UK
[2] Department of Meteorology, Reading University, UK, now at Met Office Hadley Centre, UK
[3] Centre for Ecology and Hydrology, OX, UK

The role of ecosystem-atmosphere interactions in simulated Amazonian precipitation decrease and forest dieback under global climate warming

R. A. Betts[1], **P. M. Cox**[1], **M. Collins**[2], **P. P. Harris**[3], **C. Huntingford**[3], and **C. D. Jones**[1]

With 10 Figures

Received March 13, 2003; revised September 1, 2003; accepted October 10, 2003
Published online May 6, 2004

Summary

A suite of simulations with the HadCM3LC coupled climate-carbon cycle model is used to examine the various forcings and feedbacks involved in the simulated precipitation decrease and forest dieback. Rising atmospheric CO_2 is found to contribute 20% to the precipitation reduction through the physiological forcing of stomatal closure, with 80% of the reduction being seen when stomatal closure was excluded and only radiative forcing by CO_2 was included. The forest dieback exerts two positive feedbacks on the precipitation reduction; a biogeophysical feedback through reduced forest cover suppressing local evaporative water recycling, and a biogeochemical feedback through the release of CO_2 contributing to an accelerated global warming. The precipitation reduction is enhanced by 20% by the biogeophysical feedback, and 5% by the carbon cycle feedback from the forest dieback. This analysis helps to explain why the Amazonian precipitation reduction simulated by HadCM3LC is more extreme than that simulated in other GCMs; in the fully-coupled, climate-carbon cycle simulation, approximately half of the precipitation reduction in Amazonia is attributable to a combination of physiological forcing and biogeophysical and global carbon cycle feedbacks, which are generally not included in other GCM simulations of future climate change. The analysis also demonstrates the potential contribution of regional-scale climate and ecosystem change to uncertainties in global CO_2 and climate change projections. Moreover, the importance of feedbacks suggests that a human-induced increase in forest vulnerability to climate change may have implications for regional and global scale climate sensitivity.

1. Introduction

The Hadley Centre coupled climate-carbon cycle model HadCM3LC (Cox et al., 2000) includes a submodel of vegetation dynamics and ecosystem-atmosphere carbon exchange. When driven by the IPCC IS92a emissions scenario, HadCM3LC simulates major losses of forest cover in the Amazon Basin over the next 50–100 years. The model simulates a large decrease in precipitation over much of Amazonia, initiated by an El Niño-like pattern of sea-surface warming in the Pacific Ocean (Cox et al., this issue). Associated with this drying is a large reduction in the coverage of broadleaf tree. Across large areas of Amazonia, tree cover is either reduced to savanna proportions or replaced entirely with shrubs and grasses. In part of the basin, even grasses can no longer be supported and the simulated land cover becomes semi-desert.

Clearly, this forest ''dieback'' has catastrophic implications for the ecology and socio-economics

of Amazonia. It also potentially contributes to a major positive feedback on atmospheric CO_2 rise and global climate change (Cox et al., 2000). It is therefore vital to assess the reliability of these simulations as indicators of actual future change. Such an assessment requires an understanding and quantification of the processes involved in the climate and vegetation change, so that the importance of uncertainties in representing different components of the system can be established.

This paper examines a number of mechanisms through which the forest itself contributes to the simulated precipitation changes. Both feedback and forcing mechanisms are examined. While a feedback modifies the changes initiated by an external perturbation, a forcing is the direct perturbation itself. Vegetation can be involved in both kinds of contribution to climate change.

As well as exerting a radiative forcing on the climate system, increasing concentration of atmospheric CO_2 may also exert a forcing through direct effects on plant physiology. A number of studies have shown that plant stomata may open less under higher CO_2 concentrations (Field et al., 1995), which directly reduces the flux of moisture from the surface to the atmosphere (Sellers et al., 1996). This can warm the air near the surface by increasing the ratio of sensible heat flux to latent heat flux. In a region such as Amazonia where the much of the moisture for precipitation is supplied by evaporation from the land surface, reduced stomatal opening may also contribute to decreased precipitation. Although this can be partly offset by increases in leaf area (Betts et al., 1997), this offset may not be total. While it is yet to be established whether such responses are universal, it is possible that rising CO_2 concentrations could therefore exert two forcings on Amazonian precipitation; (i) radiative forcing of global climate modifying atmospheric circulation patterns, and (ii) physiological forcing modifying near-surface temperature and also reducing the supply of moisture for precipitation. The possible relative importance of these two potential forcings on Amazonian precipitation is compared here.

However, the two forcings exerted by CO_2 may result in different impacts on the forest itself. While the radiative forcing will affect ecosystems only indirectly via climate, the physiological forcing will also affect plant functioning directly through increased water use efficiency and fertilization of photosynthesis. Therefore, the two CO_2 forcings are also compared in terms of their final effects on forest dieback.

The climate of Amazonia can also be affected by changes in the extent of forest cover. Observational and modelling studies in Amazonia suggest that the nature of the land cover can significantly influence the surface energy and moisture budgets and the atmospheric circulation. Therefore, reduced forest cover resulting from decreasing precipitation could exert feedbacks on the precipitation reduction through changes in the physical properties of the land surface.

Furthermore, changes in forest cover may affect the rate of CO_2 rise and hence provide a feedback on global climate change. If the strength of the precipitation reduction relates to the magnitude of the global temperature rise, for example through the extent of El Niño-like sea-surface warming, this could act as a further feedback on precipitation changes in Amazonia. The strengths of these feedbacks are a further focus of this paper.

We examine the relative importance of the various forcings and feedbacks by using a number of simulations with varying levels of coupling between the components of the climate system. Based on the conclusions of these modelling studies, we assess the key uncertainties in the "Amazon forest dieback" model result. We also discuss the implications for direct anthropogenic impacts on the sensitivity of the forests to climate change.

2. The models

2.1 The HadCM3LC coupled climate-carbon cycle model

The model used here is a version of the 3rd Hadley Centre Climate Model (HadCM3, Gordon et al., 2000). This is an ocean-atmosphere general circulation model (GCM) which simulates the circulations of the atmosphere and oceans as driven by thermodynamic processes which are also simulated within the model. HadCM3 has been modified to include dynamic vegetation and an interactive global carbon cycle, retaining the same horizontal resolution ($2.5^\circ \times 3.75^\circ$) in the atmosphere but reducing the ocean resolution from

$1.25° \times 1.25°$ to $2.5° \times 3.75°$ to increase computational efficiency in compensation for the extra load of the prognostic carbon cycle. The Low (ocean) resolution, Carbon-cycle version of HadCM3 is termed HadCM3LC.

HadCM3LC uses the same physical parametrizations as HadCM3 in the atmosphere. Land surface processes are modelled with the MOSES2 scheme (Essery et al., 2003), which is a revised version of the MOSES scheme used in HadCM3. MOSES2 uses a ''tile'' approach to model separate energy and water fluxes for different surface types within a gridbox. Five of these tiles correspond to Plant Functional Types (PFTs), and MOSES2 also models the physiological processes of photosynthesis, respiration and transpiration for each of these PFTs on the basis of the near-surface climate and atmospheric CO_2 concentration. The difference between photosynthesis and respiration for each PFT gives the net primary productivity (NPP) which is used in conjunction with simulated soil respiration to update atmospheric CO_2.

The distribution of the PFTs is modelled with the TRIFFID Dynamic Global Vegetation Model (DGVM) (Cox, 2001), which takes the net carbon fluxes for each PFT as input and provides the fractional cover and leaf area index (LAI) of each PFT as output. These are used to determine the physical characteristics of the land surface, such as albedo, aerodynamic roughness and moisture availability. Rooting depth is prescribed to PFT-specific distribution, with the maximum rooting depth of broadleaf trees being 3 m. MOSES2 and TRIFFID therefore allow both biogeophysical and biogeochemical (carbon cycle) feedbacks between the terrestrial biosphere and the atmosphere.

The ''HadOCC'' ocean carbon cycle model (Palmer and Totterdell, 2001) simulates the physical and biological flows of carbon within the ocean and between the ocean and atmosphere. The atmospheric CO_2 concentration is calculated within the model, rather than being prescribed from external data as is standard in other climate models. Simulations of climate change with HadCM3CL can therefore be used to examine the impacts of climate change on land and ocean ecosystems and carbon stores, and the consequent feedbacks on climate change itself (Cox et al., 2000). It is also possible to disable selected components of the model, in order to examine the nature and importance of feedbacks.

2.2 The TRIFFID dynamic global vegetation model

TRIFFID (''Top-down Representation of Interactive Foliage and Flora Including Dynamics'', Cox, 2001) models vegetation at the scale of GCM gridboxes which typically cover 50,000–100,000 km^2. Like other DGVMs, TRIFFID represents global vegetation in terms of PFTs, the current version using the five PFTs of broadleaf tree, needleleaf tree, C3 grass, C4 grass and shrub. These PFTs generally differ in their impact on the physical properties of the land surface, for example with trees, shrubs and grasses exhibiting different aerodynamic roughness lengths. The PFTs also differ in their functional responses to climate and atmospheric CO_2; for example, the two grass PFTs undergo different biochemical pathways of photosynthesis.

The distribution of the PFTs is modelled in terms of their relative coverage of each GCM gridbox. Several PFTs can co-exist in the same gridbox, each covering part of the land surface within that box. The PFTs are modelled as populations, with the fractional cover of the PFT being considered equivalent to the population size. The NPP provided by MOSES2 is partitioned into leaf, wood and root biomass per unit area, along with a component for ''spreading'' which results in a change in the fractional cover of the PFT. This spreading component implicitly represents both the change in area covered by individuals as they mature and the increase in the number of individuals through reproduction. The proportion of NPP allocated to spreading ranges from 0 at low LAI to 1 at high LAI, on the grounds that in a more mature population (with high LAI) individuals will have a smaller net uptake of carbon themselves but be more reproductive than a less mature population (with low LAI).

Spreading is countered by disturbance and by competition for light from other PFTs. Competition between tree PFTs depends on their relative canopy heights, as does competition between grass PFTs. Competition between trees, shrubs and grasses is represented in terms of a simple tree-shrub-grass dominance hierarchy.

All forms of natural disturbance, such as disease, fire and herbivory, are represented with a prescribed disturbance rate which is uniform for a given PFT. Climatic effects on disturbance, for example through fire, are not considered in this version of the model.

The fractional cover of a given PFT is therefore the outcome of the balance between NPP, the prescribed disturbance rate and the prescribed or height-dependent competition from other PFTs. Since disturbance rates are uniform, changes in cover can only result from changes in NPP or changes in height relative to certain other PFTs. This point is important when considering the mechanisms of dieback below.

Anthropogenic disturbance is represented with a land-use mask imposed as a constraint on the vegetation dynamics. Trees and shrubs are excluded from the deforested or cultivated fraction of the gridbox, and only grasses are permitted. Grasses therefore implicitly also represent crops in this version of the model.

TRIFFID therefore allows a number of types of vegetation to make up the surface within a GCM gridbox. This co-existence of several vegetation types therefore makes full use of the tile approach used by MOSES2 to represent land surface heterogeneity. Moreover, gradual changes in the fractional cover of the PFTs lead to smooth transitions in vegetation cover, unlike the sudden discontinuities which would arise from representing only ''dominant'' PFTs or biomes.

TRIFFID includes a single pool of soil carbon, and models soil respiration with a ''q_{10}'' formulation in which the respiration rate is assumed to double for every 10 K warming (i.e. $q_{10} = 2$) (Raich and Schlesinger, 1992).

The interactions with the atmosphere take place on a number of timescales. NPP and soil respiration (and hence the surface-atmosphere carbon fluxes) are calculated by MOSES2 on every 30-minute timestep of the atmospheric GCM. Leaf turnover is calculated once per day, while NPP is aggregated as input to the vegetation dynamics which is calculated on a 10-day timestep. The physical properties of the land surface are updated every day, to account for the daily changes in LAI and the 10-daily changes in PFT fractional cover.

3. Simulations of present-day vegetation

An important test of a coupled climate-vegetation model is its ability to reproduce present-day vegetation patterns. Such a test is currently the best available means of validating changes in vegetation distribution under climate change, since there is currently little data quantifying large-scale changes in natural vegetation cover over decadal and century timescales. If the model can be shown to represent observed spatial relationships between climate and vegetation, it seems reasonable to assume that it can maintain these relationships as climate changes in time.

The IGBP-DIS land cover dataset (Loveland and Belward, 1997) provides one means of validating present-day vegetation patterns. This classifies vegetation at 1 km resolution on the basis of AVHRR retrievals, and the definitions of the IGBP-DIS classes can be used to infer the maximum and minimum coverage of the TRIFFID PFTs in each IGBP-DIS class. These can therefore be used to derive maps of the maximum and minimum fractional coverage of the TRIFFID PFTs at the GCM scale, against which the model output can be objectively compared. If the IGBP-DIS dataset can be considered to be ''ground-truth'', these PFT fractions provide error bounds for the present-day simulation. If the fractional cover of a given PFT is simulated to be between the maximum and minimum coverage inferred from the IGBP-DIS dataset, the model simulation is consistent with satellite observations.

In a HadCM3LC simulation driven with pre-industrial CO_2 and near-current agricultural land use, large expanses of evergreen broadleaf tree are successfully simulated around the Equator (Fig. 1). Both the Amazonian and Central African forests are largely within IGBP-DIS bounds (Fig. 2), and tree cover also agrees with IGBP-DIS in the less disturbed parts of the Indonesian archipelago. In the equatorial regions, any overestimation of tree cover coincides with the presence of crop classes in IGBP-DIS. The dataset used to derive the anthropogenic disturbance mask (Wilson and Henderson-Sellers, 1985) included little or no agriculture in these regions, so any errors in the equatorial regions arise largely from the disturbance mask rather than the vegetation dynamics. The exception to this is near

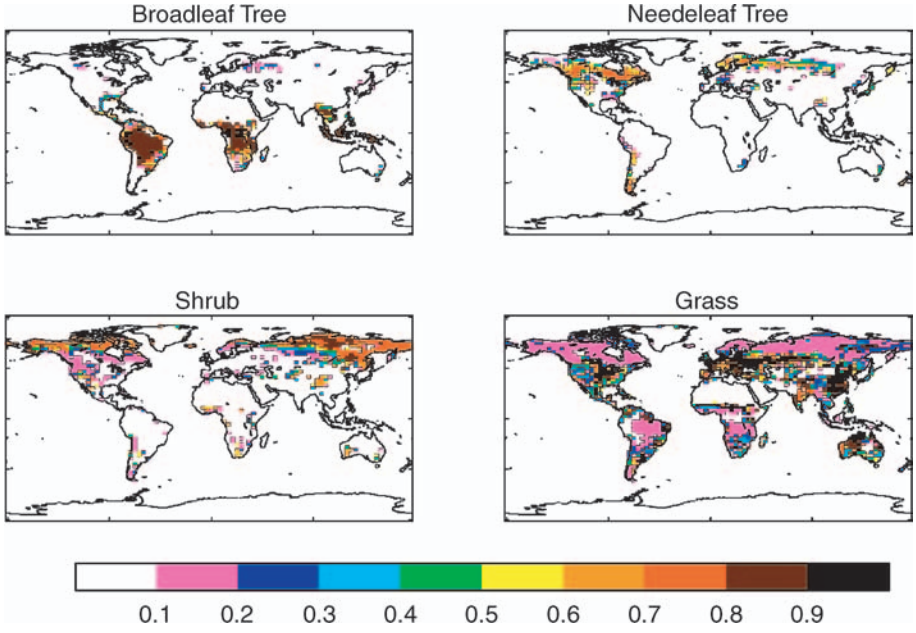

Fig. 1. Fractional coverage of plant functional types simulated by the HadCM3LC pre-industrial control simulation

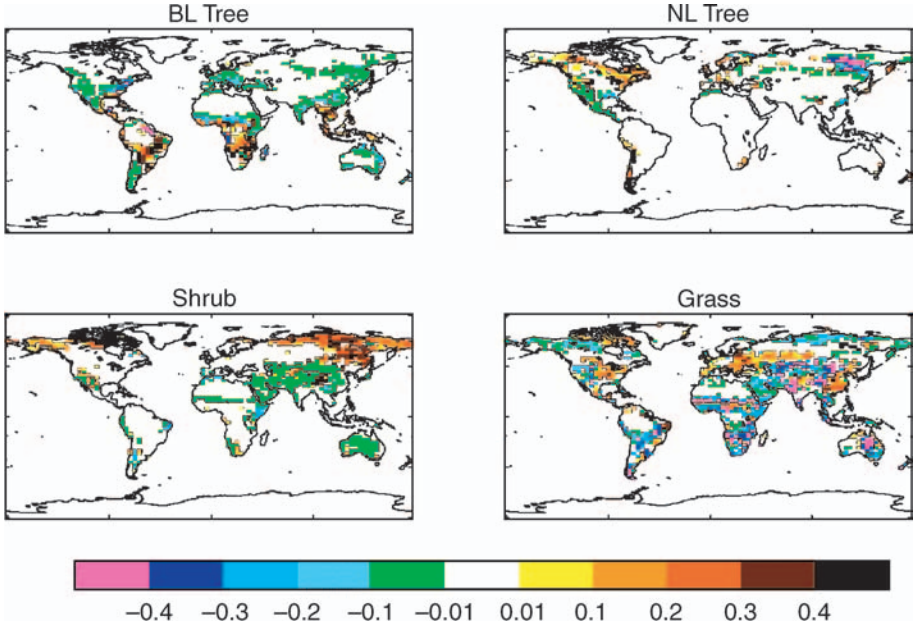

Fig. 2. Comparison of HadCM3LC PFT fractions with those inferred from the IGBP-DIS land cover dataset

the mouth of the River Amazon, where five gridboxes are covered largely by C4 grass instead of broadleaf tree. This is due to the atmospheric model simulating too little precipitation in comparison with an observed climatology (Cox et al., this issue; Harris et al., this issue), a feature which seems to be common to a number of GCMs. It is speculated that a poor representation of orography leads to a systematic under-prediction of precipitation. Such a bias may be exacerbated by land-atmosphere-ocean interactions at the coast (C.M. Taylor, personal communication).

It is also noted that, with the exceptions noted above, the model reproduces the longitudinal variations in tree cover in the equatorial regions. The observed sparser coverage east of Amazonia and east of the Congo basin is successfully simulated. Overall, then, the simulated density and extent of equatorial forest cover agrees well with IGBP-DIS (Fig. 2).

Deserts and regions of sparse vegetation are also well-positioned by the model, and in particular, the Sahara desert is simulated as almost completely barren in agreement with IGBP-DIS.

However, in some of these regions the simulated vegetation is too sparse. For example, the boundary of the Sahara with the Sahel is 3°–5° to the south of that observed. A similar under-representation of semi-arid shrub and grass cover is seen in south-west Africa, central and south-west Asia, south-west North America, and Australia.

In savanna regions apart from the Sahel, simulated tree cover is higher than the maximum inferred from IGBP-DIS (Fig. 2). This is likely to be due to inadequate treatment of ''natural'' disturbance mechanisms such as fire – while TRIFFID includes a spatially-explicit treatment of disturbance through deforestation, other disturbances are crudely represented with a uniform disturbance rate that is independent of climate or local land use practices. Frequent fire is an important feature of savanna landscapes, so neglecting fire could lead to large underestimates of local disturbance rates and the over-prediction of tree cover in savanna regions. However, it is noted that the simulated NPP for broadleaf trees in savanna regions is lower than in equatorial forests, indicating an appropriate gradient of productivity away from the Equator.

The simulation of vegetation patterns in the wet and dry tropics and sub-tropics provides an important guide to the robustness of the vegetation response to changes in tropical precipitation regime. Since HadCM3LC successfully simulates dense, productive broadleaf forest in the equatorial forests, less productive tree cover in the savannas and grasslands, shrublands and semidesert in the drier regions, it appears that the relationships between simulated vegetation and climate in the tropics is good. This seems to suggest that vegetation responses to a drying climate ought to be robustly simulated by TRIFFID.

The response of the simulated carbon cycle to climate variability may also provide some validation of the terrestrial biosphere response to climate change. Jones et al. (2001) compared the simulated and observed variability in atmospheric CO_2, focussing on relationships with the El Niño-Southern Oscillation (ENSO). The variability of Pacific sea-surface temperatures (SSTs) and global mean CO_2 simulated by HadCM3LC was found to agree well with observations. This indicated a good simulation of the interannual variability in both the physical climate and the global carbon cycle. In a study exploring a range of possible values of q_{10} for soil respiration (Jones and Cox, 2001) it was found that with this model the best agreement with the observed CO_2 variability is achieved with $q_{10} = 2.1$. This is close to the value of $q_{10} = 2$ used in the present study.

Amazonia is seen to become a source of carbon in El Niño events in HadCM3LC. The atmospheric component of HadCM3LC has been shown to reproduce the observed teleconnections between sea-surface temperatures and Amazonian precipitation during ENSO events (Spencer and Slingo, 2003), so the contribution of the simulated Amazonian ecosystem to ENSO-related CO_2 variability should result from an appropriate climate variability in the region. These results suggest that HadCM3LC simulates a qualitatively realistic response of Amazonian ecosystems to climate variability including ENSO.

4. Simulated future changes in Amazonian climate and forest cover

In a HadCM3LC simulation from 1860 to 2100 driven by historical emissions and the IS92a emissions scenario, the global mean temperature rises by approximately 5 K with mean land temperature increasing by 8 K (Cox et al., 2000). An El Niño-like pattern of sea surface temperature change increases in intensity as global temperatures rise, and precipitation over Amazonia decreases consistently. The annual mean precipitation rate over Amazonia falls from approximately 5 mm day^{-1} in the pre-industrial state to approximately 2 mm day^{-1} by 2100 (Fig. 3). At some gridpoints in the north-east of Amazonia, precipitation reaches almost zero by the end of the 21st Century.

The drought and the rising temperatures lead to a decrease in the NPP simulated for broadleaf trees. Less carbon is therefore available for spreading, but the prescribed disturbance rate remains constant. The result is a decrease in the fractional coverage of broadleaf tree (Fig. 4), not through an increase in disturbance but through a decreased opposition of disturbance by spreading. The decrease begins in north-eastern Amazonia and spreads westwards and southwards. At points where the drying becomes extreme, NPP becomes negative causing the carbon-related rate of spread

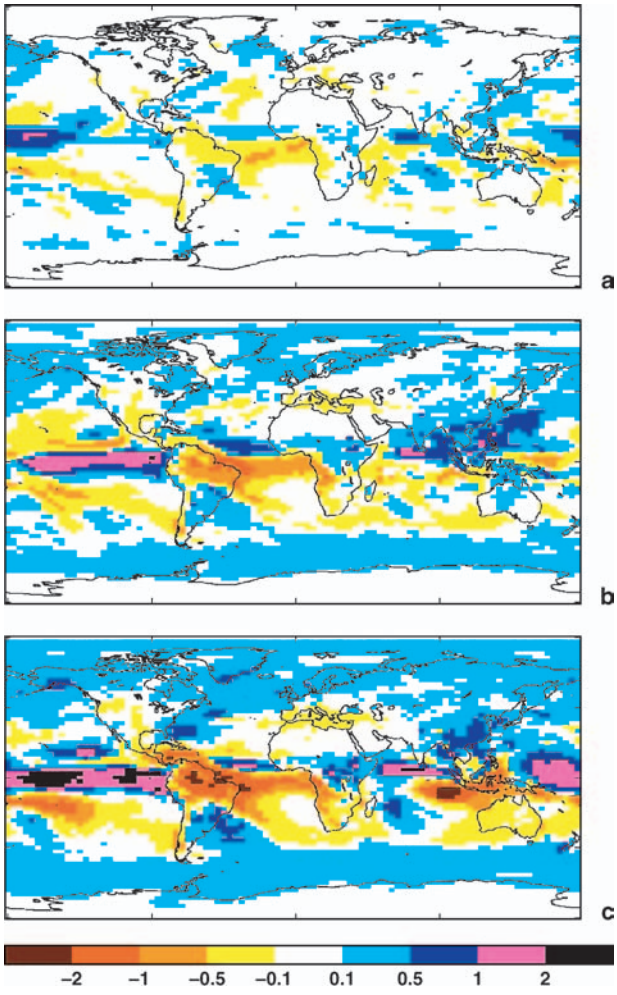

Fig. 3. Simulated changes in precipitation (mm day^{-1}) relative to 2000. 30-year means centred around (**a**) 2020, (**b**) 2050 and (**c**) 2080

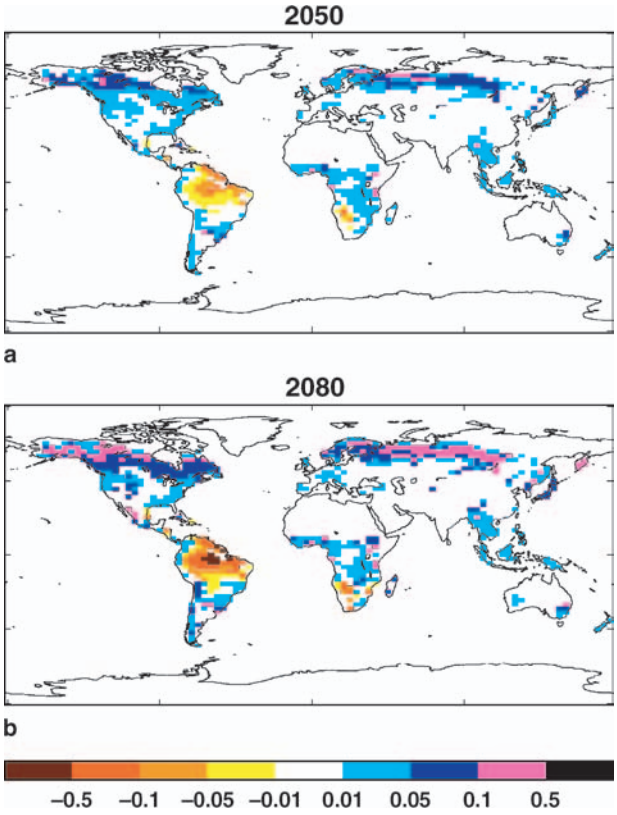

Fig. 4. Simulated changes in fractional cover of the broadleaf tree functional type relative to 2000. 30-year means centred around (**a**) 2050 and (**b**) 2080

to become negative, i.e. a reduction in area covered by the population. This is analogous to increased mortality under increased environmental stress, and provides a further reduction in the fractional coverage in addition to the fixed disturbance rate. At locations where NPP becomes negative, dieback therefore proceeds rapidly.

As broadleaf tree cover recedes, its competitive constraint on the spread of the shrub and grass PFTs is reduced. The shrubs and grasses are therefore able to spread in the place of the forest. Eventually, conditions in some locations become unfavourable even for shrubs or grasses and their own NPP reduces. Again, the decreasing NPP and fixed disturbance rate lead to a reduction in cover, and in the driest gridboxes the bare soil is largely left exposed. By the end of the 21st Century, the mean broadleaf tree coverage of Amazonia has reduced from over 80% to less than 10%. In approximately half of this area, the trees have been replaced by C4 grass leading to a savanna-like landscape. Elsewhere, even grasses cannot be supported and the conditions become essentially desert-like.

5. Investigating the roles of vegetation in Amazonian climate change

This paper examines the extent to which the simulated drying and dieback is influenced by three interactions between the Amazon forest and climate:

i) Feedbacks on climate via changes in land surface properties (“biogeophysical feedbacks”)
ii) Feedbacks on climate via the carbon cycle
iii) Physiological forcing of climate and vegetation by increasing CO_2, in comparison with radiative forcing

Table 1. Forcing and feedback elements of the HadCM3LC simulations

Simulation	CO_2 concentration	CO_2 forcing	Other GHGs	Vegetation
FIXVEG	Prescribed	Rad & physiol	IS92a	Fixed
DYNVEG	Prescribed	Rad & physiol	IS92a	Dynamic
CCYCLE	Interactive	Rad & physiol	IS92a	Dynamic
CNORAD	Interactive	Physiol	Fixed	Dynamic
RAD	Prescribed	Rad	Fixed	Dynamic
RADPHYS	Prescribed	Rad & physiol	Fixed	Dynamic

Each interaction is examined with a pair of climate change simulations with HadCM3LC, each simulation enabling or disabling a particular component of the climate system (Table 1). The simulations are of climate change under the IPCC IS92a scenario of 21st Century greenhouse gas emissions and/or concentrations.

Simulations FIXVEG and DYNVEG are used to examine the effects of biogeophysical feedbacks on climate change. Both simulations model climate change from 1870 to 2100 with atmospheric CO_2 and other greenhouse gases (GHGs) prescribed to a time-dependent concentration history and projection. From 1870 to 2000, CO_2 and the other GHGs are prescribed to the observed or reconstructed global mean concentrations. From 2000 to 2100, CO_2 and the other GHGs are prescribed to the concentrations projected by the IPCC under the IS92a scenario. FIXVEG uses vegetation fixed at the pre-industrial state as previously simulated by HadCM3LC, while simulation DYNVEG allows vegetation to respond to the climate change and alter the land surface properties. Comparison of DYNVEG and FIXVEG therefore shows the effect of biogeophysical feedbacks on climate change.

In both FIXVEG and DYNVEG, anthropogenic land use was fixed at the initial state as defined from the observed dataset (Wilson and Henderson-Sellers, 1985). Past and future changes in anthropogenic disturbance, such as those arising from deforestation, are therefore not included. Any changes in vegetation cover simulated by DYNVEG therefore arise purely from vegetation responses to climate change.

Simulation CCYCLE also models climate from 1870 to 2100, and also includes dynamic vegetation. However, whereas DYNVEG used an externally-prescribed CO_2 concentration scenario, the atmospheric CO_2 concentration in CCYCLE is simulated within the model taking account of the impacts of the changing climate on the components of the carbon cycle. The driving variable for CCYCLE is therefore the documented or reconstructed emissions for 1870–2000, and anthropogenic CO_2 emissions projected by IS92a scenario for 2000–2100. Since the IS92a CO_2 concentration scenario prescribed in FIXVEG and DYNVEG did not account for changes in climate, comparison of CCYCLE with FIXVEG and DYNVEG shows the effect of climate-carbon cycle feedbacks on climate change.

In order to place the carbon cycle changes in CCYCLE in context with those previously projected with ''offline'' carbon cycle models neglecting climate change, a further simulation CNORAD is performed with an interactive carbon cycle but with the radiative (''greenhouse'') effect of CO_2 disabled. This then gives projections of changes in atmospheric, oceanic and terrestrial carbon under the IS92a emissions scenario and with rising CO_2 directly fertilizing vegetation productivity, but with no account taken of radiatively-forced climate change.

In CCYCLE and CNORAD, emissions from land use are prescribed as a direct input to the atmospheric CO_2 budget, rather than being derived from a land use scenario being applied to the vegetation dynamics. As in DYNVEG, the constraint on vegetation distribution due to land use remained fixed at the initial state, so land use change exerted an impact via the carbon cycle but not via changing land surface properties.

Simulations RAD and RADPHYS are used to compare the radiative and physiological forcings by rising CO_2. These simulations were initialised at the year 2000 state simulated by DYNVEG, and the IS92a CO_2 concentration scenario from 2000 to 2100 was applied to the radiative transfer

scheme in both models. However, only in RADPHYS was this CO_2 rise applied to the plant physiology scheme. In RAD, the CO_2 concentration applied to the plant physiology scheme was fixed at the year 2000 concentration throughout the run. Both simulations included dynamic vegetation. The differences between RADPHYS and RAD therefore show the effects of physiological CO_2 forcing when applied in conjunction with radiative forcing. This difference can be compared with the changes in RAD to determine its importance relative to the radiative forcing alone.

Since the inclusion of radiative forcings by other GHGs would have prevented a direct comparison of the radiative and physiological forcings by CO_2, RAD and RADPHYS only included changes in CO_2. The concentrations of other GHGs were fixed at those defined for the year 2000 through both RAD and RADPHYS.

6. An additional forcing of climate change: impacts of CO_2 on plant physiology and transpiration

The potential roles of CO_2-induced stomatal closure and CO_2 fertilization in Amazonian drying and dieback were investigated with simulations RAD and RADPHYS. The former included the time-varying CO_2 in only the radiative transfer scheme of the model, fixing CO_2 at present-day levels in the plant physiology scheme, so the rising CO_2 perturbed the model only through radiative forcing and exerted no physiological forcing on the vegetation. The latter simulation applied the time-varying CO_2 to both the radiative transfer and plant physiology schemes, so here the CO_2 rise exerted both radiative and plant physiological forcings on the modelled Earth System. The difference between the two simulations therefore showed the combined effects of stomatal closure and CO_2 fertilization on the changes in climate and vegetation.

Both simulations were performed with atmospheric CO_2 prescribed to the IS92a concentration scenario, rather than using the facility for simulating CO_2 within the model. This ensured that any differences between the simulations were entirely due to the physiological responses themselves and the physical effects on climate, rather than any differential feedback on CO_2 rise. It should be noted that both simulations included dynamic vegetation, so the physiological forcing could also exert an impact through changes in leaf area and vegetation distribution. This is important, because such changes in vegetation structure may affect climate through changes in land surface properties as well as through stomatal closure. The differences between the two simulated climates therefore arise from physiological impacts on plant stomata, leaf area and vegetation distribution.

CO_2 was the only variable applied as a forcing of the simulation. Other greenhouse gases were fixed at present day concentrations. This enabled the effects of radiative forcing by CO_2 to be directly compared with the effect of combined radiative and physiological forcing, without any of the complications of additional forcings.

RAD and RADPHYS showed marked differences in precipitation in many regions across the globe by the end of the 21st Century (Fig. 5). Over Amazonia, both simulations featured a decrease in precipitation relative to the present-day (Table 2), but RADPHYS simulated a greater

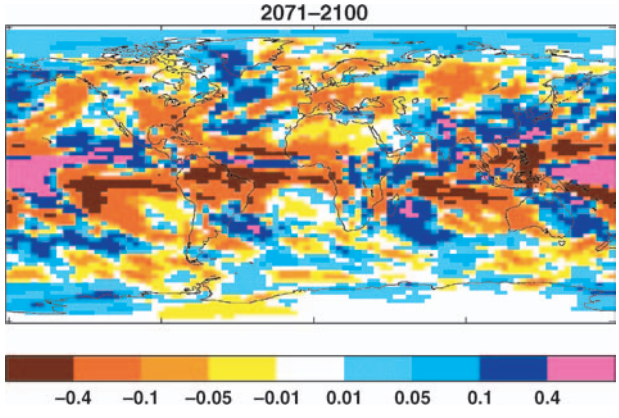

Fig. 5. Effect of physiological forcing on global precipitation patterns. Difference in precipitation (mm day^{-1}), RADPHYS – RAD. 30-year mean centred around 2085

Table 2. Mean precipitation at 2080 and change relative to 2000 in simulations without and with physiological forcing by CO_2

	RAD	RADPHYS
Precipitation in 2080s (mm day^{-1})	3.4	3.0
Precipitation change relative to pre-industrial (mm day^{-1})	−1.5	−1.9

precipitation decrease than RAD. This is consistent with a reduced evaporative return of water to the atmosphere over Amazonia, through reduced stomatal conductance (Cox et al., 1999).

However, the region of additional precipitation decrease also extends over the Atlantic ocean, suggesting that other processes may be influencing the change in precipitation patterns. The coherent large-scale patterns of precipitation increase and decrease across the globe in RADPHYS relative to RAD (Fig. 5) are indicative of differences in the global atmospheric circulation, which may have arisen from different rates of land surface warming in the two simulations. The generally lower rate of transpiration in RADPHYS leads to greater warming over land in this simulation compared to RAD (Sellers et al., 1996; Betts et al., 1997; Cox et al., 1999). Since there is more land in the northern hemisphere than the southern hemisphere, a greater rate of warming over land leads to an inter-hemispheric difference in warming which would be expected to modify global atmospheric circulation. In particular, the Inter-Tropical Convergence Zone (ITCZ) might be expected to be drawn northwards by a warmer northern hemisphere, as observed in RADPHYS compared to RAD. So, some of the additional precipitation reduction over Amazonia in RADPHYS may be due in part to physiologically-forced additional warming of land surface temperature elsewhere in the world.

To identify whether a precipitation change ΔP has been induced by local evaporation change ΔE or large-scale circulation changes, the relative magnitude of ΔP and ΔE can be examined. If ΔP is less than ΔE then ΔP could be due to reduced return of moisture through E. However, if ΔP exceeds ΔE then, by conservation, ΔE cannot be solely responsible for ΔP. A simple analysis in this manner shows that ΔE is greater than ΔP in south-western Amazonia, but in north-eastern Amazonia ΔE is smaller than ΔP (figure not shown). This suggests that in RADPHYS compared to RAD, reduced moisture recyling may contribute to the precipitation reduction in south-western Amazonia. However, in north-east Amazonia the precipitation reduction is not attributable to reduced moisture recycling, and appears instead to be associated with large-scale circulation changes caused by a physiologically-forced increased warming over land.

Physiological forcing therefore contributes to reduced precipitation over Amazonia, through two mechanisms. However, since this will also involve a direct impact on vegetation growth and hence distribution, the differences in climate between RADPHYS and RAD may not directly relate the difference in vegetation dynamics. The inclusion of the direct effects of CO_2 fertilization in RADPHYS would be expected to cause gross primary productivity (GPP) to be significantly different to that simulated in RAD. Furthermore, the increased availability of water on parts of the land surface (due to a reduced loss back to the atmosphere) could also benefit the vegetation. Therefore, to see the true implications of CO_2 physiological forcing for forest dieback, the vegetation distributions in RADPHYS and RAD must be compared.

Examining the differences in the fractional cover of broadleaf tree between RADPHYS and RAD in each decade from 2040 to 2099, it is found that the forest dieback in south-western Amazonia is actually less rapid in RADPHYS despite the greater decrease in precipitation (Fig. 6). In these regions, runoff is either similar in RADPHYS and RAD or slightly higher in RADPHYS. At points where adequate water remains available in both simulations, GPP is able to respond to the enhanced CO_2 in RADPHYS and maintain a higher fractional cover of broadleaf tree in these areas in that simulation. Furthermore, less rapid decreases in the availability of water at some points in RADPHYS may also directly help to maintain the tree cover. So in the portion of Amazonia where reduced moisture recycling is thought to drive the precipitation reduction in RADPHYS compared to RAD, the resulting decrease in precipitation does not lead to reduced forest cover.

In contrast, forest loss in north-eastern Amazonia proceeds in RADPHYS at a similar or even greater rate to that in RAD (Fig. 6). Here the precipitation reduction was found to be driven predominantly by external influences, and this is too great to be offset by CO_2 fertilization and increased water use efficiency. With insufficient water available to allow the vegetation to take advantage of the higher CO_2, forest dieback in north-eastern Amazonia remains present

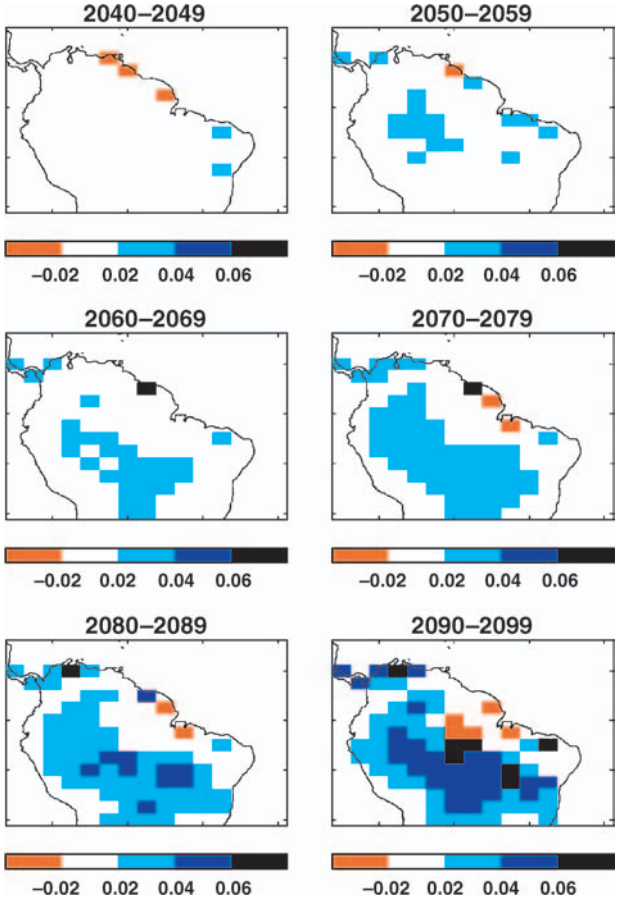

Fig. 6. Effect of physiological forcing on Amazon forest dieback. Difference in fractional cover of broadleaf tree, RADPHYS – RAD. Decadal means for 2040s to 2090s

in RADPHYS. At some points, dieback is even accelerated by the greater precipitation reductions caused by enhanced surface warming elsewhere.

Overall, then, the direct effect of CO_2 on plant physiology contributes to decreasing precipitation across Amazonia. This is due partly to reduced moisture recycling, and partly to modified atmospheric circulations arising from greater warming of the land surface under reduced transpiration. However, despite decreased precipitation, forest dieback is slowed in south-western Amazonia by enhanced vegetation productivity. In the north-east, though, where the precipitation decrease is externally-driven and most severe, dieback either remains unchanged or is increased by climatic responses to the direct effect of CO_2 on vegetation elsewhere in the world.

Amazonian precipitation decreases by approximately 30% in RAD, which includes CO_2 only as a greenhouse gas and does not include the direct effects of CO_2 on plant physiology and transpiration (Table 2). This compares with an approximately 40% decrease in RADPHYS when both radiative and physiological responses are included (Table 2). This suggests that the precipitation reduction is primarily driven by radiative forcing, with the physiological forcing of stomatal closure acting as a secondary influence.

7. Quantifying feedbacks between Amazonian drying and forest dieback

The simulations FIXVEG, DYNVEG and CCYCLE can be used together to quantify the strength of feedbacks on the simulated precipitation reduction in Amazonia. We seek to determine feedback factors for each mechanism, such that the *i*th feedback factor 'f_I' is defined as:

$$\Delta P_i = (1 + f_i)\Delta P_n \quad (1)$$

where ΔP_i is the precipitation change simulated with the *i*th feedback mechanism, and ΔP_n is the precipitation change simulated with no feedback.

7.1 Biogeophysical feedbacks

The nature of vegetation cover is a major influence on the physical properties of the land surface. In general, a forested landscape exhibits a lower surface albedo, a larger aerodynamic roughness and a greater availability of moisture for evaporation than an unforested landscape. When resulting from a large-scale change, these changes in land surface properties can significantly influence regional climates and wider-scale atmospheric circulations. The simulated widespread reduction in broadleaf tree cover in Amazonia may therefore make some contribution to the regional and global climate changes through alterations to the land surface properties.

The importance of these biogeophysical feedbacks was examined with simulations FIXVEG and DYNVEG. FIXVEG is equivalent to the typical GCM simulation currently used for climate prediction (IPCC, 2001). DYNVEG provides new feedbacks from changes in land surface properties, which have not previously been included in transient climate change simulations.

The general global patterns of climate change were similar in the two simulations, with almost all changes in temperature and precipitation being of the same sign irrespective of the inclusion of vegetation feedbacks. This implies that vegetation feedbacks are not a significant influence on atmospheric circulation in comparison with the greenhouse-gas forcing.

However, some of the regional climate changes were significantly affected by vegetation feedbacks. In particular, the precipitation reduction over Amazonia was greater in DYNVEG than FIXVEG (Fig. 7, Table 3). The main difference was in the west of the basin, where the decrease in annual mean precipitation was approximately 2.0 mm day^{-1} in DYNVEG compared to an annual mean decrease of 1.5 mm day^{-1} in FIXVEG. The mean decrease over the entire Amazon region was 2.4 mm day^{-1} in DYNVEG, compared to a decrease of 1.9 mm day^{-1} in FIXVEG.

Much of the rainfall in Amazonia is derived from water which is transported from over the oceans subject to the repeated cycling through rainfall and evaporation. Trees significantly increase evaporation by drawing up soil moisture and transpiring it through their leaves, and also by enhancing turbulent transport by increasing the aerodynamic roughness of the landscape. Reduced forest cover therefore leads to decreased evaporation and hence a diminished supply of water for further rainfall. The larger precipitation decrease in western Amazonia in DYNVEG is consistent with drought-induced dieback of the eastern forests contributing to further rainfall reductions in the west.

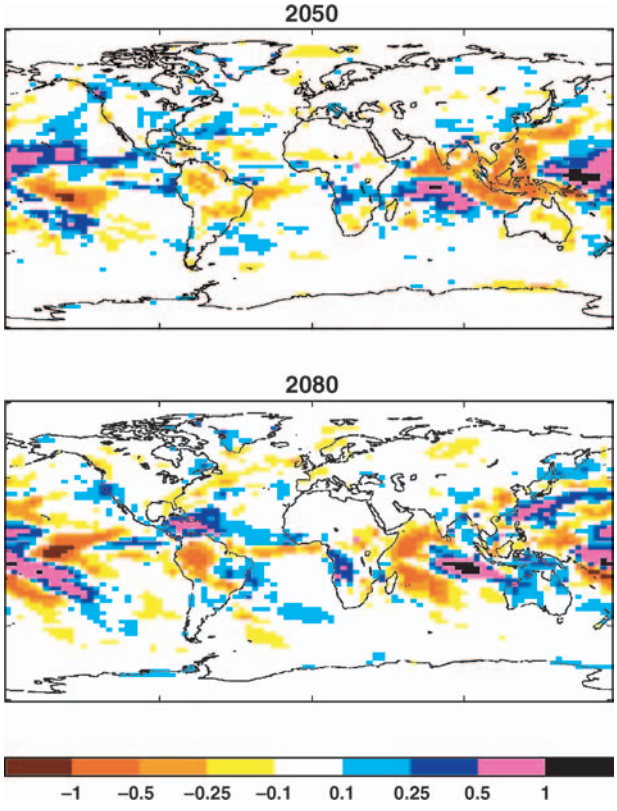

Fig. 7. Effect of biogeophysical feedback on global precipitation patterns. Difference in precipitation (mm day^{-1}), DYNVEG – FIXVEG. 30-year means centred around 2050 and 2080

Table 3. Mean precipitation at 2080 and change relative to 2000 in simulations with fixed vegetation, dynamic vegetation and an interactive carbon cycle

	FIXVEG	DYNVEG	CCYCLE
Precipitation in 2080s (mm day^{-1})	3.0	2.5	1.9
Precipitation change relative to pre-industrial (mm day^{-1})	−1.9	−2.4	−3.0
Further change relative to FIXVEG (mm day^{-1})		−0.5	−1.1

Forest loss also increases surface albedo which reduces convection and moisture convergence, which can further suppress rainfall (Charney, 1975). Albedo change may therefore be providing a further positive feedback on precipitation reduction Studies with an earlier version of the Hadley Centre model, HadCM2 (Betts, 1998) suggest that changes in evaporation provide the dominant influence of Amazon forest loss on climate, but a similar study has not yet been performed with HadCM3LC.

A biogeophysical feedback factor f_b can be defined by applying Eq. (1) to the precipitation changes simulated in DYNVEG and FIXVEG:

$$\Delta P_b = (1 + f_b)\Delta P_n \qquad (2)$$

where ΔP_b and ΔP_n are the mean precipitation changes over Amazonia from DYNVEG and FIXVEG respectively. Using the precipitation changes by 2100 (Table 1), f_b is found to be 0.26. In other words, biogeophysical feedbacks enhance the precipitation reduction by 26%.

By using this as a measure of the feedback between Amazonian precipitation reduction and

forest dieback, we assume that the difference in Amazonian climate between FIXVEG and DYNVEG is entirely due to the effects of the local vegetation change. However, since vegetation dynamics were included globally, there could also be some teleconnections from vegetation change elsewhere. For example, a slightly enhanced warming over the expanding boreal forests due to decreased surface albedo (Betts et al., 1997) could modify the global atmospheric circulation and contribute to the precipitation differences over Amazonia. Since the global patterns of precipitation difference between DYNVEG and FIXVEG are consistent in the 30-year means around 2050 and 2080, this suggests that robust global-scale changes in atmospheric circulation have taken place. However, since the additional precipitation reductions in DYNVEG appear to be localised in western Amazonia, this would appear to suggest that this particular change is associated with the local vegetation change.

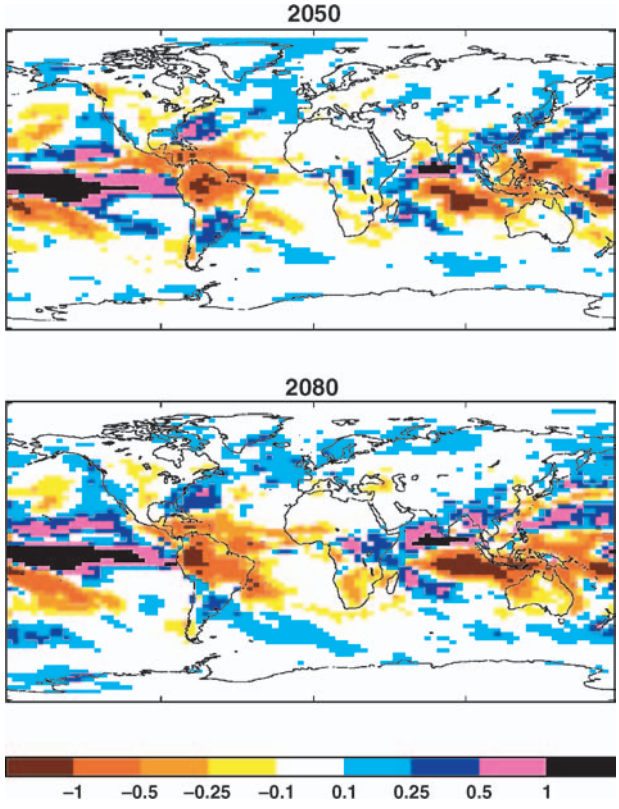

Fig. 8. Effect of including carbon cycle feedbacks on global precipitation patterns. Difference in precipitation (mm day^{-1}), CCYCLE – DYNVEG. 30-year mean centred around 2080

7.2 Carbon cycle feedbacks

Cox et al. (2000) showed that changes in net carbon fluxes from the terrestrial biosphere provided a major feedback on the climate change simulated by HadCM3LC. By comparing the prescribed-CO_2 simulation DYNVEG with a simulation including the fully-interactive carbon cycle (land, atmosphere and ocean, simulation CCYCLE), Cox et al. (2000) quantified the impacts of climate-carbon cycle interactions on atmospheric CO_2 rise and global mean. Here, further comparison between CCYCLE, DYNVEG and FIXVEG is used to examine the role of Amazonian forest carbon release on Amazonian precipitation and the forest dieback itself.

The rate of global climate warming is considerably more rapid in CCYCLE than in DYNVEG and FIXVEG, because the CO_2 rise simulated in CCYCLE is more rapid than that in the IS92a concentration scenario applied to DYNVEG and FIXVEG. The precipitation reduction over Amazonia is also greater in CCYCLE than DYNVEG (Fig. 8), the regional mean precipitation decrease being 3.0 mm day^{-1} in CCYCLE compared to 2.4 mm day^{-1} in DYNVEG and 1.9 mm day^{-1} in FIXVEG (Table 3). The combined biogeophysical and carbon cycle feedback, as represented by the difference between CCYCLE and FIXVEG, is therefore 58%.

In CCYCLE, the amplitude of the El Niño-like warming in the Pacific is enhanced in comparison with FIXVEG and DYNVEG. The amplitudes of regional precipitation changes are also greater in CCYCLE, but the global patterns of precipitation change between DYNVEG and CCYCLE are similar to the patterns of change relative to pre-industrial (compare Figs. 3 and 8). This suggests that the patterns of precipitation change associated with global warming are relatively uniform, with the local magnitudes of change varying with the strength of the warming but with few variations in the sign of local precipitation changes under different strengths of warming. However, stomatal closure and forest cover reduction are also greater in CCYCLE than in DYNVEG (Fig. 9), so the feedback will involve physiological and biogeophysical components as well as the enhancement of El Niño-like climate change.

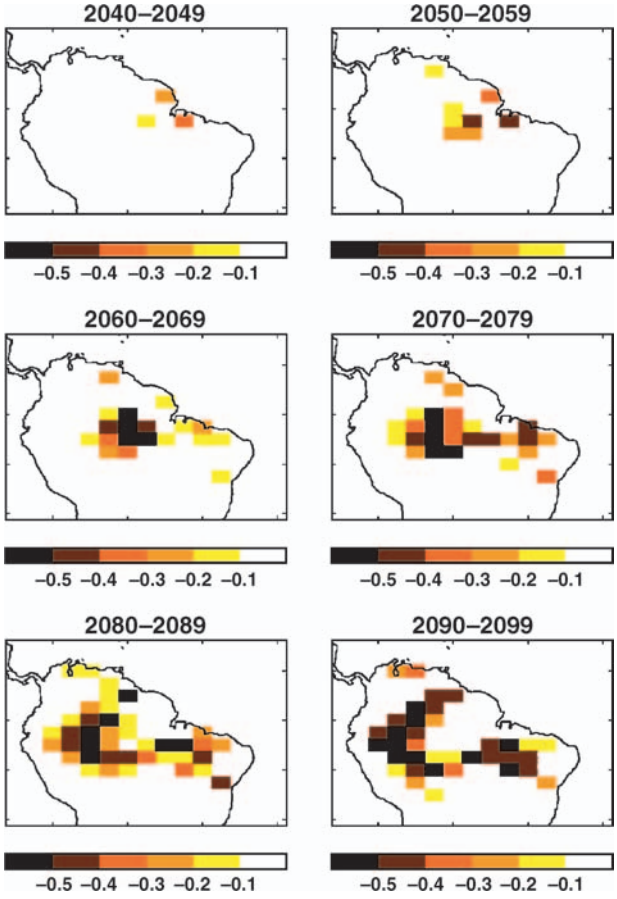

Fig. 9. Effect of including carbon cycle feedbacks on Amazon forest dieback. Difference in fractional cover of broadleaf tree, CCYCLE – DYNVEG. Decadal means for 2040s to 2090s

Comparison of the precipitation changes in CCYLE and FIXVEG therefore shows the combined impact of biogeophysical and carbon cycle feedbacks on changes in Amazonian climate. Although the differences between CCYLE and DYNVEG are due to inclusion of the interactive carbon cycle in the former, the additional changes in precipitation in CCYCLE will also partly involve biogeophysical feedbacks. Therefore, CCYCLE and DYNVEG alone cannot be used to isolate the pure carbon cycle feedback on Amazonian precipitation change – this would require a simulation including an interactive carbon cycle but no biogeophysical impacts of changes in vegetation cover, which has not been performed with HadCM3LC. However, the above estimation of the biogeophysical feedback factor f_b may be used to estimate the proportions of the combined feedback in CCCYLE vs FIXVEG attributable to biogeophysical or carbon cycle processes.

Since the carbon cycle feedbacks act on global radiative forcing while the biogeophysical feedbacks modify the regional response to this forcing, the two feedbacks can be considered to act in series. If there were a simulation with no biogeophysical feedbacks, the precipitation change ΔP_c including pure carbon cycle feedbacks f_c would be given by:

$$\Delta P_c = (1 + f_c)\Delta P_n \tag{3}$$

where ΔP_n is the mean Amazonian precipitation change in FIXVEG. With the further inclusion of biogeophysical feedbacks, the overall precipitation change ΔP_{bc} (as simulated in CCYCLE) is:

$$\Delta P_{bc} = (1 + f_b)\Delta P_c \tag{4}$$

Substituting Eq. (3) for ΔP_c in Eq. (4) gives:

$$\Delta P_{bc} = (1 + f_b)(1 + f_c)\Delta P_n \tag{5}$$

Since f_b has been estimated by comparison of DYNVEG and FIXVEG, Eq. (5) can be used to estimate the pure carbon cycle feedback factor f_c. This analysis suggests a global carbon cycle feedback of 0.25.

Since the release of carbon from the Amazonian forests is only one part of the carbon cycle feedback on climate change, quantification of the carbon cycle feedback factor for forest dieback requires comparison of the carbon release with total global impact on CO_2 rise from vegetation and soil responses to climate change. Since the analysis concerns the changes relative to FIXVEG, this comparison should be made relative to the ''offline'' carbon cycle projections applied to FIXVEG (which neglect climate-carbon feedbacks), rather than being made relative to the pre-industrial steady state. This is important because the offline projections included changes in the relative sizes of the vegetation and soil carbon pools in response to the CO_2 rise; neglecting these changes would give a misleading impression of the relative effects of climate change on each pool. These offline carbon cycle projections are replicated in simulation CNORAD, so comparison of the carbon store changes in CCYCLE and CNORAD gives the relative contributions of Amazon forest dieback and changes in global soil respiration to the overall carbon cycle feedback (Fig. 10).

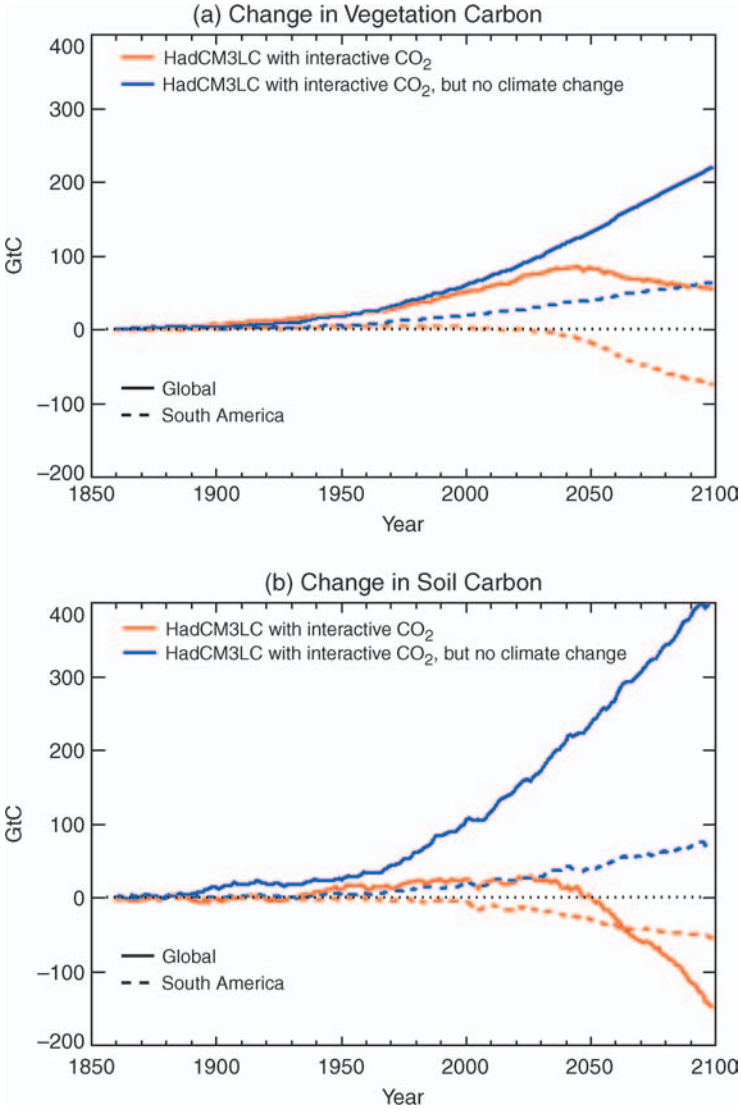

Fig. 10. Timeseries of changes in Global and South American terrestrial carbon stores with and without climate-carbon cycle feedbacks. (**a**) Vegetation carbon (**b**) soil carbon

In CCYCLE, the Amazonian forest dieback causes the above-ground carbon store in South America to reduce by 70 gigatonnes of carbon (GtC), limiting the increase in global vegetation carbon to 60 GtC. The global soil carbon store is reduced by 150 GtC (Fig. 10), mainly due to enhanced soil respiration under rising temperatures. As well as leading to forest dieback, the inclusion of climate change in CCYCLE means that the large flux of carbon into soils via increased NPP is more than offset by an increase in soil respiration under higher temperatures. This contrasts with the carbon store changes projected by CNORAD with no enhanced greenhouse effect. CNORAD projects an uptake of 60 GtC in South American vegetation, and a total uptake of 220 GtC in global vegetation and 400 GtC in global soils when the effects of climate change on the carbon cycle are neglected (Fig. 10). Therefore, relative to the increased carbon stores in CNORAD, the total terrestrial carbon deficit is 710 GtC. Of this, 130 GtC of the total deficit is due to the Amazonian forests dying back instead of becoming more productive. 550 GtC of the total deficit is due to a 150 GtC release of global soil carbon, rather than a 400 GtC uptake.

While most of the release of soil carbon globally is due to enhanced soil respiration under greenhouse warming, some of the loss of soil carbon in Amazonia will be due to forest dieback itself. Part of this will be due to reduced input of carbon from the forest, and part would be due to additional warming arising by biogeophysical feedbacks on local surface temperatures. Precise

quantification of this would require an additional simulation neglecting changes in NPP and forest cover, but it is estimated that approximately 30 GtC are lost from Amazonian soils through these mechanisms. The total loss of carbon from above and below-ground biomass attributable to forest dieback is therefore 160 GtC. Therefore, the Amazonian dieback can be considered to contribute approximately 20% to the total land feedback on atmospheric CO_2 rise in this model.

Assuming a linear relationship between CO_2 rise and Amazonian precipitation decrease, this suggests that the behaviour of the Amazonian forests as a carbon source rather than a carbon sink contributes 20% to the carbon cycle feedback factor f_c. The net carbon release from Amazonia therefore enhances the Amazonian precipitation decrease with a feedback factor of 0.05.

8. Discussion

The Amazonian precipitation reduction and forest dieback simulated by HadM3LC clearly involves a number of feedbacks and forcings, and this analysis contributes to an increased understanding of the mechanisms involved. This is useful in four ways:

i) to assist with understanding the similarities and differences in the results of the Hadley Centre models and other GCMs
ii) to provide information on aspects of the model in which uncertainties would be most important to the overall results
iii) to illustrate the potential importance of regional climate change in uncertainties in atmospheric CO_2 rise and global climate change
iv) to illustrate the potential importance of the sensitivity of Amazonian forest to regional and global climate change, and hence the importance of direct human impacts on this sensitivity.

i) Differences between the simulations of HadCM3LC and other climate models

The analysis is invaluable in explaining the differences between the predictions of this model and those of other models. Several (but not all) coupled ocean-atmosphere GCMs exhibit El Niño-like climate change and an associated precipitation reduction over Amazonia (e.g. Cai and Whetton, 2001), but the Amazonian changes simulated by HadCM3LC are the most extreme. The results presented here provide explanations for much of this extreme behaviour compared to the other models.

First, is it clear from the comparison of CCYCLE and DYNVEG that 20% of the extreme precipitation reduction in CCYLE is due simply to a more extreme global warming with carbon cycle feedbacks compared to that simulated with CO_2 prescribed to the standard IS92a concentration scenario. But in simulations driven by IS92a CO_2 concentrations, the drying is still severe. Comparison of DYNVEG and FIXVEG shows that biogeophysical feedbacks from forest loss contribute 20% to this. Comparing CCYCLE and FIXVEG (Table 3) shows that the combination of biogeophysical and carbon cycle feedbacks is responsible for 37% of the 3.0 mm day^{-1} precipitation reduction in CCYCLE. However, even ''standard'' simulations with no dynamic vegetation show major precipitation reductions over Amazonia. Not only is this the case for HadCM3LC, it is also true for the original model HadCM3 with its higher resolution ocean. Both HadCM3LC and HadCM3 include the direct effects of CO_2 on plant stomata, and comparison of RADPHYS and RAD shows that this contributes 20% to reduced Amazonian precipitation through decreased moisture recycling and altered atmospheric circulation.

None of the above processes are currently included in other GCMs used for transient climate change simulations, and all of these processes have been shown here to enhance the decrease of precipitation over Amazonia. As well as feedbacks on changes forced externally, such as a drying initiated by El Niño-like climate change, there is an additional forcing from CO_2 physiological effects. HadCM3LC and HadCM3 would therefore be expected to exhibit more extreme changes in Amazonian climate than other climate models which do not include these effects.

ii) Uncertainties in climate change simulations due to process representation

Direct validation of this result is currently difficult because there appears to have been no analogous drying event in Amazonia within the

period of reliable palaeo reconstruction. It is therefore not possible to simply use HadCM3LC to simulate the climate and vegetation of some previous drying event and test its ability to reproduce the reconstructions. So, a direct indication of the robustness of this model result is currently not available. However, the breakdown of forcings and feedbacks presented here will be useful for validating key processes represented in the model, which may ultimately contribute to assessing the robustness of the overall results.

One key uncertainty here may be the sensitivity of the forest to a warmer, drier climate. It is noted that TRIFFID only includes two tree functional types representing the main functional character of vegetation at the global scale. The inclusion of a larger number of functional types may affect the rate and character of the ecosystem change within a drying climate. For example, the forest dieback may be slowed by the spreading of functional types with greater drought tolerance due to deep rooting or deciduousness. One the other hand, climatically-related disturbances such as fire are not included this simulation, but in reality, a drier, warmer climate would be expected to increase the frequency of fire and therefore enhance the disturbance of the forest. Furthermore, increases in forest sensitivity by direct human impact are not included. Our quantification of the feedbacks will be useful in assessing the uncertainties in the result which arise from these assumptions in the vegetation model.

Another uncertainty in coupled climate-biosphere modelling is the aggregate response of canopy conductance to CO_2 rise. There is conflicting evidence regarding the generality of the stomatal closure response and the extent to which it could be offset by increasing leaf area. Again, quantification of the contribution of this mechanism to the precipitation reduction and dieback will assist with assessment of uncertainties in the simulated drying of climate.

It has been shown here that the Amazonian climate is simulated to become drier in the absence of stomatal responses to CO_2 and in the absence of biogeophysical feedbacks. Therefore, the simulated drying depends heavily on the relationship between global mean surface temperature and Amazonian precipitation patterns, a relationship which appears to depend on responses of long-term Pacific sea surface temperature. Examinations of the robustness of the Amazonian drying result should therefore include consideration of these teleconnections.

It is noted that the positive carbon cycle feedback on climate warming is predominantly due to increased soil respiration, with the Amazonian forest dieback contributing only about 20% to this feedback. This suggests that uncertainties in this positive feedback result depend mainly on the representation of soil respiration responses to temperature. Uncertainties in the simulated climate and ecosystem change in Amazonia are therefore a secondary consideration in the global carbon cycle feedback result of Cox et al. (2000).

iii) Implications of regional climate change for uncertainties in atmospheric CO_2 rise and global climate change

Despite the above observation that the carbon cycle feedback is predominantly due to soil respiration changes, the 20% contribution of Amazonian forest dieback is not negligible. Since this aspect of the result depends on regional climate change predictions which are subject to considerable uncertainty, the identification of this potential feedback to global climate implies that the uncertainties in global climate are also depend on the regional-scale uncertainties.

Comparison of CCYLE and DYNVEG can be used to illustrate the propagation of these uncertainties. For example, if mean Amazonian precipitation may plausibly decrease by between 0% and 60%, this introduces an uncertainty of 60 ppmv in the atmospheric CO_2 rise by 2100. Assuming a linear relationship between atmospheric CO_2 and global mean temperature, the range of global land warming associated with a 0%–60% reduction in Amazonian precipitation under IS92a emissions would therefore be 5 K to 5.6 K.

Clearly, while this does not imply that the uncertainties in global climate change are greater than those in regional climate change, it does imply that the uncertainties at the two scales may be more similar than previously assumed. The process of climate change is often represented as a linear cause-effect chain (GHG emissions – GHG concentrations – radiative forcing – global climate change – regional climate change – regional climate impacts) with an assumed ‘‘cascade of

uncertainty'' from high confidence in emissions to low confidence in impacts such as ecosystem responses. The importance of ecosystem feedbacks demonstrated here suggests that this ''cascade'' may have a smaller gradient than is generally assumed.

iv) The importance of Amazonian forest sensitivity to climate change

The key role of feedbacks from forest loss has major implications for the importance of the sensitivity of Amazonian forests to climate change. While the true sensitivity of the forests is still uncertain, the results presented here show that, in principle, the forest sensitivity could be a significant component of the sensitivity of regional and global climates to radiative forcing. This has implications for the long-term effects of human activity in Amazonia. Activities such as road-building, partial deforestation and selective logging have been shown to increase the climatic sensitivity of parts of the forest not directly affected by the activity. The exposure of a new forest ''edge'' can increase susceptibility to fire, and may therefore increase the sensitivity of the forest to climate change. If forest sensitivity is increased in this way, this could enhance the feedback on both regional and global climates.

9. Conclusions

The extreme 21st-Century precipitation decrease and forest dieback simulated in Amazonia by HadCM3LC is a complex, coupled process emerging from interactions between the atmosphere, the oceans and the land ecosystems of Amazonia and elsewhere.

Rising atmospheric CO_2 exerts both a radiative and a physiological forcing on the climate system, both of which contribute to decreasing Amazonian precipitation. Radiatively-forced climate change involves an El Niño-like pattern of ocean surface warming in the tropical Pacific, which has been shown elsewhere (Cox et al., this issue) to be associated with reduced rainfall in Amazonia. Physiological forcing via stomatal closure contributes approximately 20% to the precipitation decrease, acting both directly through suppressed local evaporative water recycling in Amazonia, and indirectly through enhanced warming of global land surfaces and a consequent shift in atmospheric circulation patterns. However, while stomatal closure contributes to reduced precipitation, the associated CO_2 fertilization and increased water use efficiency slows the forest dieback in the less severely-affected regions.

The forest dieback exerts two positive feedbacks on the precipitation reduction. Reduced forest cover causes further suppression of local evaporative water recycling (a biogeophysical feedback), and carbon release contributes to a global positive feedback on CO_2 rise which accelerates global warming and magnifies the associated patterns of precipitation change. The precipitation reduction is enhanced by 20% by the biogeophysical feedback, and 5% by the carbon cycle feedback from the forest dieback. The inclusion of global carbon cycle feedbacks, including soil respiration change, enhances Amazon drying by 25%.

This analysis helps to explain why the Amazonian precipitation reduction simulated by HadCM3LC is more extreme than that simulated in other GCMs. In the fully-coupled climate-carbon cycle simulation, approximately half of the precipitation reduction in Amazonia is attributable to a combination of physiological forcing and biogeophysical and global carbon cycle feedbacks. These are generally not included in other GCM simulations of future climate change.

The importance of the feedbacks from decreased forest cover has important implications for uncertainties in climate change projections. The regional-scale climate change is subject to considerable uncertainties, and the corresponding uncertainties in ecosystem response will therefore contribute to greater uncertainties in the projections of CO_2 rise and global climate change. A further major implication of the importance of feedbacks is that direct anthropogenic impacts on the sensitivity of forests may affect regional and global climate sensitivity.

It is concluded that the simulated Amazon precipitation reduction and forest dieback is comprised of a number of forcing and feedback processes which all act to increase the climatic drying. Despite the lack of a previous analogue climate for whole-system validation, the individual processes appear to be physically plausible. Further work is urgently required on quantifying the uncertainties associated with the processes

identified here. While these results should not be viewed as a prediction, the analysis to date suggests that under increasing concentrations of CO_2 and other greenhouse gases, a transition to a drier, less forested Amazon cannot be ruled out.

Acknowledgements

We thank John Gash, Jose Marengo, Carlos Nobre, Chris Taylor, Keith Williams, Ning Zeng and an anonymous referee for informative discussions on the model results. RAB was supported in this work by the EU Project "PROMISE". The work of RAB, PMC and CDJ forms part of the Climate Prediction Programme of the UK Department of the Environment, Food and Rural Affairs (contract PECD 7/12/37). MC, PPH and CH were supported by the UK Natural Environment Research Council.

References

Betts RA (1998) Modelling the influence of the vegetated land surface on climate and climate change. PhD thesis, University of Reading, UK

Betts RA, Cox PM, Lee SE, Woodward FI (1997) Contrasting physiological and structural vegetation feedbacks in climate change simulations. Nature 387: 796–799

Cai W, Whetton PH (2001) A time-varying greenhouse warming pattern and the tropical-extratropical circulation linkage in the Pacific Ocean. J Clim 14: 3337–3355

Charney JG (1975) Dynamics of deserts and droughts in the Sahel. Quart J Roy Meteor Soc 101: 193–202

Cox PM, Betts RA, Jones CD, Spall SA, Totterdell IJ (2000) Acceleration of global warming due to carbon-cycle feedbacks in a coupled climate model. Nature 408: 184–187

Cox PM (2001) Description of the TRIFFID dynamic global vegetation model. Technical Note 24, Hadley Centre, Met Office

Cox PM, Betts RA, Collins M, Harris P, Huntingford C, Jones CD (2004) Amazonian dieback under climate-carbon cycle projections for the 21st century. Theor Appl Climatol (this issue)

Essery RLH, Best MJ, Betts RA, Cox PM, Taylor CM (2003) Explicit representation of subgrid heterogeneity in a GCM land-surface scheme. J Hydromet 4: 530–543

Field C, Jackson R, Mooney H (1995) Stomatal responses to increased CO_2: implications from the plant to the global scale. Plant, Cell Environ 18: 1214–1255

Gordon C, Cooper C, Senior CA, Banks H, Gregory JM, Johns TC, Mitchell JFB, Wood RA (2000) The simulation of SST, sea ice extents and ocean heat transports in a version of the Hadley Centre coupled model without flux adjustments. Clim Dyn 16: 147–168

Harris PP, Huntingford C, Gash JHG, Hodnett M, Cox PM, Malli Y, Aranjo AC (2004) Calibration of a land-surface model using data from primary forest sites in Amazonia. Theor Appl Climatol (this issue)

IPCC (2001) Climate Change 2001: The Scientific Basis. Contribution of Working Group I to the Third Assessment of the Intergovernmental Panel on Climate Change. Cambridge University Press, 881 pp

Palmer JR, Totterdell I (2001) Production and export in a global ocean ecosystem model. Deep-Sea Res 48: 1169–1198

Jones CD, Collins M, Cox PM, Spall SA (2001) The carbon cycle response to ENSO: A coupled climate-carbon cycle model study. J Clim 14(21): 4113–4129

Jones CD, Cox PM (2001) Constraints on the temperature sensitivity of global soil respiration from the observed interannual variability in atmospheric CO_2. Atmospheric Science Letters, doi: 10.1006/asle.2001.004

Loveland TR, Belward AS (1997) The IGBP-DIS global 1 km land cover dataset, Discover: first results. Int J Remote Sens 18: 3289–3295

Sellers PJ, Bounoua L, Collatz GJ, Randall DA, Dazlich DA, Los SO, Berry JA, Fung I, Tucker CJ, Field CB, Jensen TG (1996) Comparison of radiative and physiological effects of doubled atmospheric CO_2 on climate. Science 271: 1402–1406

Spencer H, Slingo JM (2003) The simulation of peak and delayed ENSO teleconnections. J Clim 16(11): 1757–1774

Wilson MF, Henderson-Sellers A (1985) A global archive of land cover and soils data for use in general circulation climate models. J Climatol 5: 119–143

Authors' addresses: R. A. Betts (e-mail: richard.betts@metoffice.com), P. M. Cox and C. D. Jones, Hadley Centre for Climate Prediction & Research, Met Office, Exeter EX1 3PB, UK; M. Collins, Department of Meteorology, Reading University, UK; P. P. Harris and C. Huntingford, Centre for Ecology and Hydrology, OX10 8BB, UK.